June 1971

Raising of Discrete Levels into the Far Continuum

J.L. Dehmer
University of Chicago, Chicago, Illinois

Anthony F. Starace
University of Nebraska-Lincoln, astarace1@unl.edu

U. Fano
University of Chicago, Chicago, Illinois

J. Sugar
National Bureau of Standards, Washington, D. C.

J.W. Cooper
National Bureau of Standards, Washington, D. C.

PHYSICAL REVIEW
LETTERS

VOLUME 26 | 21 JUNE 1971 | NUMBER 25

Raising of Discrete Levels into the Far Continuum*

J. L. Dehmer,† A. F. Starace,‡ and U. Fano
Department of Physics, University of Chicago, Chicago, Illinois 60637

and

J. Sugar and J. W. Cooper
National Bureau of Standards, Washington, D. C. 20234
(Received 26 April 1971)

Broad peaks observed in the photoabsorption spectra of rare earths ~10-20 eV above the $4d$ edge are attributed to transitions $4d^{10}4f^N \rightarrow 4d^9 4f^{N+1}$. Exchange interaction splits the $4d^9 4f^{N+1}$ configuration and raises some multiplets by ~20 eV. Autoionization to $4d^9$-$4f^N \epsilon f$ broadens the high levels. The interpretation extends to $p \rightarrow d$ processes observed in the absorption of synchrotron light by transition elements.

This Letter points out and interprets a curious coexistence of discrete and continuum features in the absorption spectra of rare earths near the $N_{IV,V}$ ($4d$-electron) threshold, i.e., in the range of 100- to 200-eV photon energies. These features have emerged from experimental studies with elements from Sn ($Z = 50$) to Lu ($Z = 71$).[1,2] For $Z < 57$ one observes primarily a high broad peak 20 or more eV above threshold, with an integrated oscillator strength of ~10 electrons. From La ($Z = 57$) through Ho ($Z = 67$) there is a main peak 5 to 20 eV above threshold, with *variable structure,* variable width (5 to 25 eV), and *decreasing strength* with increasing Z; numerous weak lines also appear near the threshold. Only the lines remain from $Z = 68$ to $Z = 70$ and no feature has been detected at $Z = 71$.

Centrifugal effects associated with $d \rightarrow f$ transitions ($d \rightarrow p$ having low intensity) are known to have a major influence on these spectra. For $Z < 57$ a centrifugal potential barrier of 10-20 eV keeps low-energy f orbits outside the region of space where the $4d$ orbits are confined. Accordingly, $4d \rightarrow f$ transitions become intense only at energies sufficiently high to permit the f-electron's wave function to penetrate inside the barrier, thus overlapping the $4d$ wave function.[3,4] [In other words, the escaping electron must receive sufficient energy to surmount the barrier.] For $Z \geq 57$, on the other hand, the $4f$ orbit has a small radius which fits inside the centrifugal barrier, while f orbits with somewhat higher energy remain well outside. One would then expect to observe intense $4d \rightarrow 4f$ transitions in the rare earths while transitions to $5f$ and high discrete levels and to the low-energy f continuum remain suppressed by the barrier.[5]

This expectation is supported by experimental evidence for the analogous case of $3d$ photoabsorption, which shows for Xe a broad maximum well above each of the $M_{IV,V}$ edges,[6] but for rare earths a single, dominant $3d \rightarrow 4f$ line below each edge.[7] Experimentally, though, $4d$ photoabsorption by the rare earths peaks well *above* threshold. The main task of our interpretation of rare earth spectra thus lies in demonstrating how the optical spectrum of $4d \rightarrow 4f$ transitions may peak above the ionization threshold.

Rare earth atoms in the metallic (or oxidized) state are generally trivalent.[8] Hence their spectra are characteristic of a triply (sometimes doubly or quadruply) ionized core from which $6s$ or

$5d$ electrons have been effectively removed. Accordingly we regard the $4d \rightarrow 4f$ spectrum as consisting of transitions from the ground level of a $4d^{10}4f^{N}$ configuration to the numerous levels of a $4d^{9}4f^{N+1}$ configuration. The key point is that these latter levels are spread over a very broad range of $\gtrsim 20$ eV, primarily by the effect of exchange interaction between the f electrons and the d vacancy. Sample calculations show most of the oscillator strength to be concentrated in transitions to the higher levels of $4d^{9}4f^{N+1}$, when the $4f$ shell is not nearly filled. These levels lie far above threshold and hence autoionize rapidly, mainly to the configuration $4d^{9}4f^{N}\epsilon f$.

The large role of exchange interaction between vacancies and electrons of unfilled subshells has also been demonstrated by other experiments.[9] This interaction is stronger between subshells with equal than with different principal quantum number n, and hence affects $4d \rightarrow 4f$ more than $3d \rightarrow 4f$ transitions. Note that the analogous exchange interaction represented by the integral $R^{1}(4d\epsilon f, \epsilon' f 4d)$ broadens the peak of the Xe ($Z = 54$) spectrum and raises its energy further.[10] The same exchange interaction yields the pair correlations that underlie the phenomenological collective-model theories and their prediction of unexpected peaks in photoabsorption continua.[11] Here we also attribute continuum peaks to effects of electron interaction but within the framework of conventional atomic theory; this framework yields not only detailed quantitative predictions but a rich structure in the spectrum of $4d \rightarrow 4f$ transitions.

Interpretation of rare earth spectra in terms of $4d \rightarrow 4f$ transitions also accounts directly for the observed decrease of $4d$ oscillator strength along the sequence of elements from $Z = 57$ to 71. In particular, the $4d \rightarrow 4f$ transition is forbidden by the exclusion principle for $Z \geq 71$; in general, its total strength is proportional to the number of vacancies in the $4f$ subshell in accordance with a sum rule to be discussed elsewhere. [Reduction and eventual disappearance of absorption peaks upon filling of outer shells had been commented upon in Ref. 4, but without any real explanation.]

The preceding discussion and interpretation of rare earth spectra may extend to any optical transition whose final state depends critically on a centrifugal barrier. We have particularly in mind the absorption by $3p$ electrons in transition elements[12] whose features are analogous to those of $4d$ rare earth spectra, though less pronounced; these features should result from $3p \rightarrow 3d$ transitions.[13]

To develop our interpretation into a detailed quantitative treatment, spectroscopic theory is combined with the existing theory[14] of multilevel, multichannel autoionization. The complete theory, to be reported elsewhere, resolves into a network of partial calculations. Results of a few preliminary calculations are described below for purposes of illustration.

The effect of a centrifugal barrier upon the penetration of f- (or d-) electron orbits expresses itself in the values of matrix elements for transitions to or from such orbits; in particular it is illustrated by the dependence of such matrix elements upon the energy of the orbit under consideration. Figure 1 shows the spectral distributions of matrix elements for optical transition and for electrostatic dipole exchange interaction, illustrating particularly the rapid change of this distribution with increasing Z when the radius of the $4f$ (or $3d$) orbit contracts to fit within the atomic radius. The spectra of Fig. 1 pertain to matrix elements that constitute input data for a detailed theory of the photoabsorption spectrum. Note the large values of the exchange integrals R^{1} for the discrete ground state orbits in Ce and V.

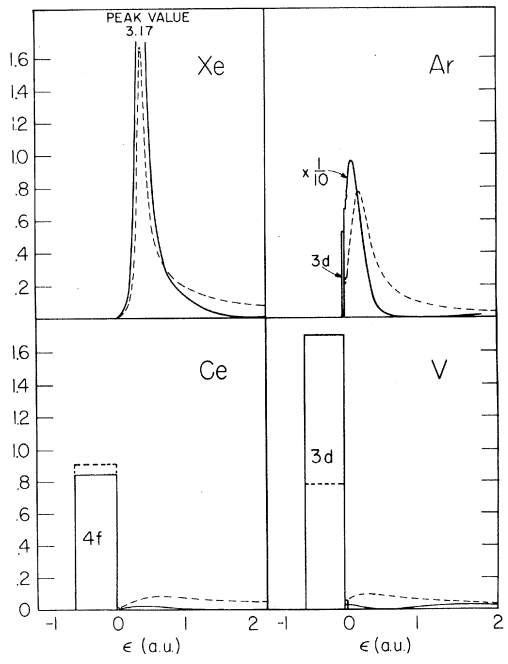

FIG. 1. Independent electron model matrix elements for Ar and V ($nl = 3p, l' = 2$), and for Xe and Ce ($nl = 4d$, $l' = 3$. Solid line, $|(nl|r|\epsilon l')|^{2}$ (a.u.); dashed line, $R^{1}(nl\epsilon l'; \epsilon l' nl)$ (dimensionless).

Table I. Comparison of observed and calculated energy levels in La, Ce, Er, and Tm. State designations represent the largest LS component in each level and should be considered as labels rather than as assignments. Level intervals only are calculated, their absolute scale being adjusted for each element. The fitted parameter values for Ce are $F^2 = 10.6 \pm 1.6$ eV and $G^1 = 10.1 \pm 0.3$ eV.

Element	Initial State	Prime Final States	E_{calc}(eV)	E_{ob}(eV)
La	$4d^{10}\,{}^1S_0$	$4d^9 4f\,{}^3P_1$	97.1	96.9
	"	" $^3D_1$	101.3	101.6
	-	-	-	103.7
	"	" $^1P_1$	117.7	117.
Ce A	-	-	-	101.27
B	$4d^{10}4f\,{}^2F_{5/2}$	$4d^9 4f^2\,{}^2G_{7/2}$	103.5	103.5
C	"	" $^4G_{5/2}$	104.5	104.6
D	"	" $^4G_{7/2}$	105.8	105.8
E	"	" $^4G_{5/2}$	106.1	106.1
F	"	" $^4H_{7/2}$	106.8	106.6
G	"	" $^4D_{3/2}$	108.3	108.1
H	"	" $^4D_{5/2}$	108.6	108.9
J	"	" $^4F_{7/2}$	109.9	109.7
K	"	" $^4H_{7/2}$	110.3	110.4
L	"	" $^2G_{7/2}$	111.8	111.5
Levels above the ionization limit	"	" $^2G_{7/2}$	120.4	121.5
	"	" $^2F_{5/2}$	125.3	124.3
	"	" $^2D_{3/2}$	124.4	
	"	" $^2D_{5/2}$	124.7	
	"	" $^2F_{7/2}$	125.3	
Er	$4d^{10}4f^{11}\,{}^4I_{15/2}$	$4d^9 4f^{12}\,{}^4K_{17/2}$	164.2	163.4
	"	" $^4H_{13/2}$	164.9	165.1
	"	" $^4I_{15/2}$	167.3	167.2
	"	" $^4H_{13/2}$	174.2	174.8
Tm	$4d^{11}4f^{12}\,{}^3H_6$	$4d^9 4f^{13}\,{}^3H_6$	171.6	171.6
	"	" $^3H_5$	175.1	174.6
	"	" $^3G_5$	178.1	178.5

Matrix elements evaluated (like those of Fig. 1) with central-field[15] wave functions were utilized to calculate for La^{3+} the sequence of optical and autoionization transitions

$$4d^{10}(^1S_0) \rightarrow 4d^9 4f(^3P_1, ^3D_1, ^1P_1) \rightarrow 4d^9 \epsilon f.$$

The resulting absorption spectrum agrees qualitatively with the experiment[1] (if one considers also a $4d \rightarrow 6p$ transition) but its main peak lies higher in energy and is sharper than observed. This discrepancy is not unexpected, since high-order perturbations are known to be very important in rare earth spectra and to reduce the level splits calculated by low-order procedures[16]; our results (not shown) were in fact improved by partial evaluation of high-order effects. This diffi-

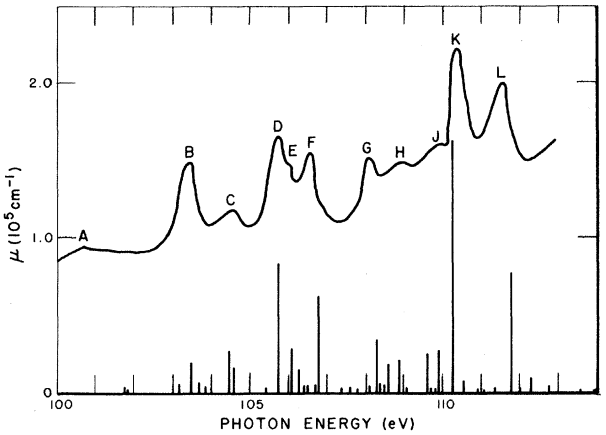

FIG. 2. Comparison of μ, the measured absorption coefficient for Ce in the region of the $N_{IV,V}$ edge from Ref. 2, with the calculated relative positions and line strengths of $4d^{10}4f\ ^2F_{5/2} \rightarrow 4d^9 4f^2$ transitions. Additional line positions corresponding to prominent peaks in the ionization region are shown in Table I.

culty was bypassed by empirical adjustment of key interaction parameters in separate, more detailed calculations of discrete $4d^9 4f^{N+1}$ levels.

Figure 2 shows a comparison between calculated levels of $4d^9 4f^2$ ($J = \frac{3}{2}, \frac{5}{2}, \frac{7}{2}$)—with predicted line strengths for the transitions from the $4d^{10}4f\ ^2F_{5/2}$ of Ce^{3+}—and the experimental spectra of Ref. 2 for Ce metal ($Z = 58$). The calculation started from the energy matrix of the $4d^9 4f^2$ configuration, for each J value, written in terms of direct (F^2, F^4) and exchange (G^1, G^3, G^5) Slater integrals and spin-orbit parameters (ζ_d, ζ_f). Spin-orbit parameters were obtained from experimental data[17] and initial estimates of Slater parameters from Hartree-Fock (HF) calculations.[18] Each matrix was then diagonalized to predict energy levels. The values of F^2 and G^1 were finally adjusted to optimize agreement with Ref. 2, keeping the $F^2{:}F^4$ and $G^1{:}G^3{:}G^5$ ratios at their HF values. The eigenvectors of each matrix served to transform relative line strengths for the array from their LS-coupling values to the coupling of the predicted levels.

Figure 2 does not extend to the main levels far above the ionization threshold. More extended data for Ce are given in Table I along with results obtained by similar calculations for La, Er, and Tm. The latter calculations were performed without least-square adjustment of calculation of line strengths, the HF values of the Slater parameters being reduced in the same ratios as for Ce. We regard the overall agreement of the theoretical and experimental data in Fig. 2 and Table I as confirming the analysis presented in this Letter. In addition, we have obtained for Ce a value of ~50:1 for the line strength ratio of all the five levels of Ce above the ionization threshold to those below it. The integrated oscillator strength in the experimental data appears to be >20:1 but is difficult to estimate from Ref. 2.

---

*Work supported by U. S. Atomic Energy Commission, Contract No. COO-1674-45.

†National Science Foundation Trainee, Department of Chemistry.

‡National Science Foundation Graduate Fellow.

[1]T. M. Zimkina, V. A. Fomichev, S. A. Gribovskii, and I. I. Zhukova, Fiz. Tverd. Tela 9, 1447, 1490 (1967) [Sov. Phys. Solid State 9, 1128, 1163 (1967)]; T. M. Zimkina and S. A. Gribovskii, to be published.

[2]R. Haensel, P. Rabe, and B. Sonntag, Solid State Commun. 8, 1845 (1970).

[3]J. W. Cooper, Phys. Rev. Lett. 13, 726 (1964).

[4]U. Fano and J. W. Cooper, Rev. Mod. Phys. 40, 441 (1968).

[5]The disappearance of oscillator strengths of $4d \rightarrow \epsilon f$ transitions for $Z \gtrsim 57$ in single-electron model calculations has been noted by F. Combet-Farnoux, C. R. Acad. Sci., Ser. B 246, 1728 (1967).

[6]R. D. Deslattes, Phys. Rev. Lett. 20, 483 (1968).

[7]F. H. Combley, E. A. Stewardson, and J. E. Wilson, J. Phys. B: Proc. Phys. Soc., London 2, 120 (1968); H. F. Zandy, Phys. Rev. 162, 1 (1967); K. C. Williams, Proc. Phys. Soc., London 87, 983 (1966); E. A. Stewardson and J. E. Wilson, Proc. Phys. Soc., London 69, 93 (1956); H. F. Zandy, Proc. Phys. Soc., London 65, 1015 (1952).

[8]See, e.g., L. Brewer, to be published.

[9]C. S. Fadley and D. A. Shirley, Phys. Rev. A 2, 1109 (1970).

[10]A. F. Starace, Phys. Rev. A 2, 118 (1970); M. Ya. Amusia, N. A. Cherepkov, and L. V. Chernysheva, Zh. Eksp. Teor. Fiz. 60, 160 (1971) [Sov. Phys. JETP, to be published].

[11]See, e.g., W. Brandt, L. Eder, and S. Lundqvist, J. Quant. Spectrosc. Radiat. Transfer 7, 185 (1967); M. Ya. Amusia, N. A. Cherepkov, and S. I. Sheftel, Phys. Lett. 24A, 541 (1967).

[12]B. Sonntag, R. Haensel, and C. Kunz, Solid State Commun. 7, 597 (1969); see also R. Haensel, K. Radler, B. Sonntag, and C. Kunz, Solid State Commun. 7, 1495 (1969), for the analogous $O_{II,III}$ spectra.

[13]Considerations analogous to ours have been developed by Prof. A. P. Jucys for the rare earths and by Dr. E. J. McGuire for the transition elements, according to private communications.

[14]U. Fano, Phys. Rev. 124, 1866 (1961); F. H. Mies, Phys. Rev. 175, 164 (1968).

[15]F. Herman and S. Skillman, *Atomic Structure Calculations* (Prentice-Hall, Englewood Cliffs, N. J., 1963).

[16]B. G. Wybourne, *Spectroscopic Properties of Rare*

Earths (Interscience, New York, 1965), Sect. 2-18.
[17]W. T. Carnall, P. R. Fields, and K. Rajnak, J. Chem. Phys. 49, 4424 (1968); J. A. Bearden, Rev. Mod. Phys. 39, 78 (1967).
[18]These calculations are based on the code of C. Froese. See Can. J. Phys. 41, 1895 (1963).

Hydrodynamics of Nematic Liquid Crystals*

Huey-Wen Huang
Department of Molecular Biophysics and Biochemistry, Yale University, New Haven, Connecticut 06520
(Received 21 April 1971)

The Ericksen-Leslie theory for nematic liquid crystals is simplified and improved. The most general linear hydrodynamic equations are obtained following the conservation laws, thermodynamics laws, and symmetry properties. The rigorous low-frequency, long-wavelength equations are then deduced by taking such a limit. It is a simple alternative way to derive the theory of Forster, Lubensky, Martin, Swift, and Pershan. It would be of interest to study the more general equations experimentally.

The hydrodynamic theory of nematic liquid crystals has been discussed by many authors.[1-5] Most recently Forster, Lubensky, Martin, Swift, and Pershan[6] (FLMSP) have derived the low-frequency, long-wavelength equations for the case of zero external field. In this note we rederive the FLMSP theory by simplifying and improving the Ericksen-Leslie theory.[3,7] We discard unnecessary assumptions such as the transformation properties between noninertial frames of reference. Following the conservation laws, thermodynamics laws, and symmetry properties, we obtain the *most general* set of linear hydrodynamic equations. The rigorous low-frequency, long-wavelength equations are then obtained by taking such a limit. Our more general equations are, however, subject to experimental test.

The macroscopic description of the state of a nematic liquid crystal is effected by means of the local density ρ, velocity $\vec{v}$, pressure p, and unit vector $\hat{n}$ denoting the orientation of the molecular axis. In this note, we shall neglect thermal expansion and conduction.

The conservation of mass is expressed by

$$d\rho/dt = -\rho\partial v_i/\partial x_i. \tag{1}$$

(A summation from 1 to 3 is implied for repeated indices.) The stress tensor σ_{ij} is defined by the conservation of translational momentum:

$$(d/dt)\int_V \rho v_i\, dV = -\oint_A p\, dA_i + \oint_A \sigma_{ij}\, dA_j, \tag{2}$$

where V denotes any material volume with surface boundary A and dA_i the vector component of a surface element. In Eq. (2) a potential force has been neglected because it is of second order in variations.[1,3]

We define the angular velocity of a molecular axis to be

$$\omega_i = \epsilon_{ijk} n_j^0 \partial n_k/\partial t \simeq \epsilon_{ijk} n_j^0 dn_k/dt \tag{3}$$

with corresponding moment of inertia per unit mass I_i; $\hat{n}^0$, the equilibrium nematic direction, is taken to be the 3 axis. Under the assumption that $I_1 = I_2 = I$ while $I_3 \sim 0$, the conservation of angular momentum in the 1 and 2 directions can be written as

$$(d/dt)\int_V (\rho\epsilon_{ijk} x_j v_k + \rho I\omega_i) dV = -\int_V \epsilon_{ijk} n_j^0 (dF/dn_k) dV - \oint_A p\epsilon_{ijk} x_j\, dA_k + \oint_A \epsilon_{ijk} x_j \sigma_{kl}\, dA_l + \oint_A \Gamma_{ij}\, dA_j, \tag{4}$$

where F is the potential energy per unit volume including that due to the external field,[2,4] and the torque tensor Γ_{ij}, which is defined by this equation, balances the other torques. Whether Γ_{ij} exists or not can only be determined by experiment. Equation (4), which is second order in time, can be regarded as the single-collision-time modification[8] of the FLMSP equation for ω_i.

From Eqs. (2) and (4), one obtains the equation for rotation of the molecular axis:

$$\rho I d\omega_i/dt = -\epsilon_{ijk} n_j^0 dF/dn_k - \epsilon_{ijk}\sigma_{jk} + \partial\Gamma_{ij}/\partial x_j. \tag{5}$$